V. Dj. Vukić: Rapid and Long-Term Gamma-Radiation Annealing in ...
Nuclear Technology & Radiation Protection: Year 2017, Vol. 32, No. 2, pp. 155-165

155

RAPID AND LONG-TERM GAMMA-RADIATION ANNEALING IN LOW-DROPOUT VOLTAGE REGULATORS

by

Vladimir Dj. VUKIĆ[*]

Institute of Electrical Engineering "Nikola Tesla", University of Belgrade, Belgrade, Serbia

Samples of four types of low-dropout voltage regulators, with both serial pnp and npn transistors, were examined in room-temperature isothermal gamma radiation annealing. After uninterrupted exposure to a total ionising dose of 500 Gy, biased and loaded voltage regulators were examined in room-temperature annealing within the first 30 minutes after the exposure. Beside the on-line measurement of output voltage and quiescent current during the thirty-minute period immediately after irradiation, also results were procured after 10-year room-temperature spontaneous recovery. Data obtained during the irradiation and rapid annealing were fitted with linear, exponential, and power-law regression functions. A simple procedure was proposed, based on the quiescent current annealing factor, for the quick estimation of the integrated voltage regulator's radiation sensitivity during the post-irradiation isothermal annealing. In order to estimate the circuit's radiation sensitivity, immediately after irradiation, tested devices have to be left in the same operating conditions as during the exposure. If a clear trend of the quiescent current recovery can be observed, further examinations have to be implemented to estimate if a circuit is acceptably radiation-tolerant. If no recovery trend can be observed within the first hour after irradiation, or even further degradation is noticed, then the examined voltage regulator is a radiation-sensitive device and cannot be used in radiation environments. The described procedure is based on the macroscopic effects of the radiation-induced charge-trapping in field oxides and interfaces.

Key words: voltage regulator, gamma radiation, quiescent current, annealing factor, isothermal annealing, post-irradiation effect, regression analysis

INTRODUCTION

Analogue bipolar integrated circuits (ICs) are very important components in any electronic equipment used in nuclear or space radiation environments. The main effects observed in linear bipolar circuits are related with the loss of the bipolar transistor's forward emitter current gain, as well as the establishment of radiation-induced leakage currents [1, 2]. These effects are primarily created owing to the generation of radiation-induced interface traps and the oxide-trapped charge in elementary bipolar transistors [1]. However, the effects of the described trapped charge may be significantly reduced during the circuit's recovery, yet their negative influence may also increase the damage created during the irradiation process [2]. Accordingly, it is very important to estimate the devices' recovery already during the tests of integrated circuits, prior to their implementation in electronic devices made for a radiation environment.

The electronic devices recovery process after irradiation is usually described with the term "annealing"

[1]. Despite this word's suggestion that the recovery process must be executed in an elevated ambient temperature, in fact this is not the case. Irradiated circuit annealing may be performed at temperatures both high above and far below room temperature (usually 20 °C) [2]. Therefore, if the annealing is performed at a constant temperature, this process can be described as isothermal annealing [1]. On the other hand, recovery in a predefined time interval, with various ambient temperatures, represents the isochronal annealing process [1, 2].

In previous years, many authors have analysed annealing in silicon semiconductor devices [3-17]. The main focus was on research of annealing in MOS transistors and integrated circuits [4-7, 11-15], yet considerable attention was also paid for the time-dependent radiation effects in bipolar devices and related field oxides [3, 8, 10]. Radiation response of an integrated circuit is very complex, being affected by the characteristics of its transistors (MOSFET or bipolar, silicon or heterojunction, etc.), mutual influence of its elementary circuits, as well as a type of implemented ionising radiation, its dose rate, then temperature, bias conditions, load, etc. While MOSFET in integrated circuits are primarily affected by the radiation re-

156

V. Dj. Vukić.: Rapid and Long-Term Gamma-Radiation Annealing in ...
Nuclear Technology & Radiation Protection: Year 2017, Vol. 32, No. 2, pp. 155-165

sponse of their thin, high-quality gate oxides, bipolar transistors are strongly affected by the radiation effects in thick and contaminated field oxides. Thus, while an integrated circuit's response is strongly affected by the elementary mechanisms of charge trapping in oxides and interfaces, their influence cannot be simply predicted.

For the variety of applications, from space to nuclear and military, it is very important to perform preliminary tests in laboratory conditions, in order to determine the electronic devices' radiation tolerance. Yet laboratory conditions differ significantly from the real exploitation conditions, particularly in terms of the ionising radiation dose rate (from Gys^{-1} in the Earth orbit, up to MGys^{-1} in a military nuclear environment [2]). Also, laboratory tests usually last for several hours or, at most, several weeks [1]. This is in sharp contrast to the exploitation period of approximately 100 000 hours that is common for electronic components designed for operation in space or an accelerator radiation environment [1]. Therefore, in order to properly estimate the radiation damage, it is very important to normalise the results of laboratory tests on the real exploitation interval and the environment. In a long exploitation period, not only instant radiation effects would be present, but also dose-rate and time-dependent post-irradiation effects. These time-dependent effects may lead to both the circuit's recovery and its further degradation. So, it is not enough only to estimate the device's radiation tolerance during the ionising radiation exposure, but also its post-irradiation trend, i. e., annealing or deterioration.

For estimation of the post-irradiation effects, one approach is to repeat the analysis of the laboratory samples after their 10-year storage, and compare it with the initial annealing data set. The purpose of the implemented procedure is to estimate the circuit response after exposure and evaluate its post-irradiation trends, related to the trapped charge in oxides and interfaces. An idea derived in this paper was to evaluate the alternative method for procurement of the annealing factor in integrated low-dropout voltage regulators, with both serial pnp and npn power transistors.

THEORY

Radiation annealing represents the partial or total removal of the ionising radiation effects on electronic devices. After irradiation, most of the defects generated in the semiconductor recombine at room temperature after several hours [1]. On the other hand, annealing of the oxide-trapped charge may vary significantly, in the range from hours to years [4]. The oxide-trapped charge concentration may increase rapidly with total ionising dose, having the dominant effect in the initial phase of irradiation. On the other hand, interface trap generation is much slower, and, during the

irradiation, may significantly compensate the effects of the oxide-trapped charge. While the oxide-trapped charge may anneal significantly even at room temperature, particularly during the initial phase of recovery, build-up of the interface states may continue during longer periods after irradiation [17]. As many authors have written before [4, 12, 17], positive charge in the oxide, particularly radiolytic hydrogen-related ions and species, as well as the hydrogen molecules existing in the electronic device package well before irradiation, tend to move toward the Si-SiO$_2$ interface. On that interface, positive charge may react with atoms of silicon, creating bonds and increasing the concentration of interface traps [4]. In n-channel MOS transistors (and parasitic MOS structures in field oxides of bipolar circuits), interface traps have negative signs, being opposite to the total oxide-trapped charge [7].

The principal differences in radiation effects in electronic devices are based on the great variations in the dynamics of the interface traps and the oxide-trapped charge generation [4]. Depending on the device type, geometry, technological process implemented and materials, macroscopic radiation effects may differ significantly. This is also the case with radiation annealing.

Beside the temperature and total ionising dose, as well as the type of ionising radiation, bipolar transistor annealing is strongly affected by the technological parameters, such as the oxide quality, concentration of impurities and the geometry of the elementary transistors. Isothermal annealing was thoroughly analysed in MOSFET. Detailed experiments pointed to the dominant influence of tunnel annealing at room temperature, while for elevated temperatures (above 75 °C-100 °C) thermal emission dominates the annealing in oxides [4]. The influence of the interface traps and the oxide-trapped charge differs significantly. While the oxide-trapped charge anneals according to the natural logarithm as a function of time (ln$t$) [16], interface traps, in general, hardly anneal at room temperature, and may even build up further as the annealing process progresses with time [13, 17]. Nevertheless, integrated circuit recovery can never be complete (i. e., it is not possible to completely recreate the state that existed before irradiation), owing to the lasting radiation effects on the crystal structures of both semiconductor and oxide [1].

For bipolar transistors, a time-dependent annealing factor, $F(t)$, may be expressed [1, 10, 18]

$$F(t) = \frac{\beta^{-1}(t) - \beta^{-1}(0)}{\beta^{-1}(4) - \beta^{-1}(0)},$$ (1)

$$F(t) \geq 0, \quad F(0) = 1, \quad F(4) = 1$$

where $\beta(t)$ is the forward emitter current gain after elapse of time t after irradiation, $\beta(0)$ – the transistor's current gain before irradiation, $\beta(4)$ – the forward emitter current gain after an infinite recovery period.

Originally, the annealing factor was defined for the variations of the forward emitter current gain in bipolar junction transistors [18]. In order to procure reliable results, the current gain has to be recorded for constant values of the base-emitter voltage. Since all the examined circuits in the presented research are three-terminal voltage regulators, output voltage, as well as output and quiescent currents are the only output parameters that can be directly measured. Therefore, all other important parameters can only be recalculated or estimated, by either the use of other experimental results or the integrated circuit computer simulation.

In integrated circuits, the quiescent current usually represents the current of their internal consumption. In the voltage regulator, there are two basic circuit topologies that may affect the quiescent current. One is related to the serial pnp transistor and, for circuits with positive output voltage, quiescent current, I_Q, is the sum of the serial transistor's base current I_B, and the internal control circuit supply current I_{Q_0} [19]

$$I_Q \quad I_B \quad I_{Q_0} \qquad (2)$$

The other important topology is based on the serial npn power transistor. If this kind of voltage regulator has positive output voltage, the serial transistor's base current is superimposed with the serial transistor's emitter current and is therefore not related to the voltage regulator's quiescent current. Yet, if the voltage regulator with serial npn transistor has negative output voltage, the serial transistor's base current is superimposed on the internal circuit's consumption current. These differences are very important since the ionising radiation may affect the internal supply current and the serial transistor's base current in various ways [20].

Internal consumption of the control circuit in a voltage regulator may be a particularly useful measure of the voltage regulator's radiation sensitivity, since it is not affected by the circuit's negative feedback reaction, contrary to the serial power transistor's base current at a particular operation point. Usually, the internal supply current decreases with the total dose, while the serial transistor's base current increases during the exposure [20]. Nevertheless, these scenarios may vary in different devices, both qualitatively and quantitatively, compensating or superimposing each other's variation.

The idea of this research is to use the quiescent current annealing factor in order to estimate the integrated circuit's degradation. Based on relation (1), an analogy was implemented in order to create the quiescent current annealing factor, F_{I_Q}

$$F_{I_Q}(t) \quad \frac{I_Q^{-1}(t) \quad I_Q^{-1}(0)}{I_Q^{-1}(4) \quad I_Q^{-1}(0)}, \qquad (3)$$

$$F_{I_Q}(0) \quad 0, \; F_{I_Q}(4) \quad 1$$

where $I_Q(t)$ is the voltage regulator's quiescent current after elapse of time t after irradiation, $I_Q(0)$ – the quiescent current before irradiation, $I_Q(4)$ – the quiescent current after an infinite recovery period (85 000 hours in the experiment described in this paper).

Thus, it is very important to examine if the voltage regulator's quiescent current can be a reliable indicator of the circuit's degradation or recovery affected by radiation or post-irradiation effects. Also, it is necessary to find if the proposed alternative annealing factor can be used for the examination of both rapid and long-term post-irradiation effects.

EXPERIMENT

Experiments were performed on four types of low-dropout voltage regulators, with various pass transistors and implemented technological processes. Integrated 5-volt commercial off-the-shelf (COTS) low-dropout voltage regulators were tested at the Vinča Institute of Nuclear Sciences, Belgrade, Serbia, in the Metrology-dosimetric laboratory. The following devices were examined in γ-radiation fields: LM2940CT5, L4940V5, LM2990T-5 and LT1086CT5. All the examined circuits had different serial power transistors: LM2940CT5 is a classical bipolar integrated circuit with a serial lateral pnp transistor with round emitters, L4940V5 is a BiCMOS device with a serial vertical pnp transistor, LM2990T-5 is a negative voltage regulator with a serial super-β npn transistor, while LT1086CT5 is a quasi-low-dropout positive voltage regulator with a serial npn transistor. The LM2940CT5 circuits were from the batch PM44AE, made by National Semiconductor's subcontractor in China [20]. The L4940V5 devices were from the WKOOGO 408 batch, made by ST Microelectronics in China [19]. The LM2990T-5 is from batch JM45AB, made in the National Semiconductor facility in United Kingdom [21]. Finally, LT1086CT5 is a circuit made by Linear Technology, from batch 3529013. All circuits were in plastic TO-220 cases.

As a source of γ-radiation, ^{60}Co was used. The measurement of the exposition doses was performed with the cavity ionising chamber "Dosimentor" PTW M23361, using the reader DI4 [19, 20]. All current and voltage measurements, as well as the irradiation of the components, were performed at a room temperature of 20 °C [22, 23].

All devices were continuously exposed to γ-radiation, without cessation of the irradiation. The devices were irradiated until the predetermined total doses of 500 Gy were reached (with a dose rate of 4 cGys^{-1}). Therefore, irradiation in the ^{60}Co field lasted continuously for approximately three and a half hours. In order to record the annealing process immediately after irradiation, all measurements were performed within a time interval of half an hour after the exposure.

The principal quantities used for the detection of the continuously irradiated voltage regulator's degra-

158

V. Dj. Vukić: Rapid and Long-Term Gamma-Radiation Annealing in ...
Nuclear Technology & Radiation Protection: Year 2017, Vol. 32, No. 2, pp. 155-165

dation due to exposure to ionising radiation were the voltage regulator's output voltage and quiescent current [20]. During irradiation, the tested biased devices were supplied with the same input voltage, 8 V, whilst the load currents had the same value: 100 mA. During this experiment, there were no interruptions to the irradiation, with testing of additional circuits with various input voltages and output currents. Therefore, this set of data was the control ensemble, prearranged for the most faithful possible approximation of the exploitation conditions in the real radiation environment. Immediately after cessation of the exposure, the devices were tested with the same operating conditions as during the primary experiment. Every minute, the values of the voltage regulator's output voltage and quiescent current were recorded. The examined circuits remained under the same bias conditions for thirty minutes after irradiation, with the same values of input voltage and output current as was the case during the circuit's radiation exposure.

For the next 10 years after the irradiation, all the tested circuits were kept stored in the office locker, at a room temperature in the range of 15 °C-25 °C for all the intervening time. After nearly 10-year room-temperature annealing (precisely, in January 2017, 85 000 hours after the γ-radiation exposure), current and voltage measurements were done again, on exactly the same samples that were exposed to radiation with the specified bias and load.

Further details about the experiment, the implemented technological process and construction of voltage regulators can be found in [19-23].

RESULTS

After the first series of experiments on low-dropout voltage regulators, performed in 2005, data on the maximum output current and minimum dropout voltage were procured after 168-hour room-temperature recovery. Initial results pointed to a significant recovery of the maximum output current for circuits LM2940CT5, reaching 80-90 % of the pre-irradiation values [24]. Loaded voltage regulators L4940V5 and LM2940CT5 (from the 2007 series of experiments) also demonstrated recovery of the output voltage, as recorded during the control measurements several years later, being briefly described in references [19] and [22]. Thus, the author expected that, following the same trends in the years to come, 10-year room-temperature annealing would lead to the recovery of most of the oxide-trapped charge and, consequently, to the predominant recovery of the irradiated low-dropout voltage regulators to their pre-irradiation parameters. Successful recovery was in particular expected for the L4940V5 devices, which are proven radiation-tolerant circuits [19, 20], and that also demonstrated fast recovery in the initial period of post-irradiation room-temperature annealing.

However, detailed examinations performed after the 10-year room-temperature storage of the irradiated samples did not justify the initial expectations.

Figures 1-4 present the change in the voltage regulator's output voltage (left y-axis) and quiescent current (right y-axis) during the continuous irradiation up to the dose of 500 Gy. In the same figures, data were also presented that followed during the rapid isothermal annealing period (biased samples for the first 30 minutes after exposure) and, finally, data on the output voltage and quiescent current recorded after 10-year room-temperature annealing of unbiased samples. In order to present such a diverse ensemble, the x-axis is presented (linearly) as time dependence (in hours), rather than as a function of a total ionising dose (in Gy). For a dose rate of 4 cGy/s, irradiation of all samples lasted for approximately 3.5 hours, followed by the annealing period, lasting up to 85 000 hours. In figs. 1-4, the break in the x-axis is placed between 4 and 80 000 hours from the beginning of irradiation. The second part of the x-axis, after the break, is presented in logarithmic scale.

Figure 1 describes relatively wide variations of output parameters in the National Semiconductor LM2940CT5 circuit, a low-dropout voltage regulator with a lateral serial pnp power transistor. Figure 2 indicates the stable output voltage and clear exponential increase in the quiescent current of the L4940V5 voltage regulator, a BiCMOS circuit with a vertical serial pnp power transistor. At first sight, fig. 3 is nearly the same as fig. 1, but there is a big difference in the output voltage trend, since LM2990T-5 is a negative voltage regulator, and, therefore, the output voltage absolute value does not have a rising trend (as in fig. 1), but a sharply declining one. The output parameters of the
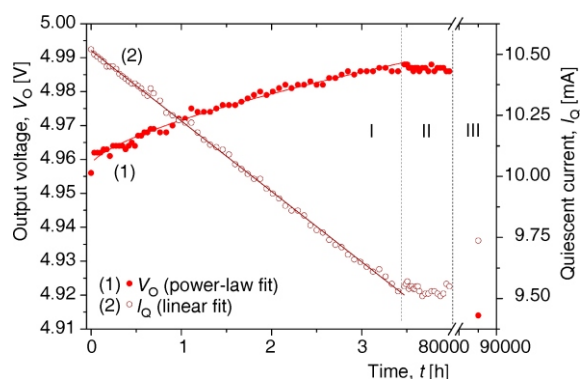

Figure 1. Change in the output voltage and quiescent current in the biased and loaded ($V_{in} = 8$ V, $I_{out} = 100$ mA) voltage regulator LM2940CT5, under the influence of γ-radiation (area I), followed by the first half an hour after the exposure to γ-radiation (area II), complemented with additional data on 85 000-hour room-temperature annealing without bias (area III); variations of the output voltage during irradiation were successfully fitted with the allometric power-law regression function, eq. (4); variations of quiescent current during irradiation were successfully fitted with a linear regression function, eq. (5)
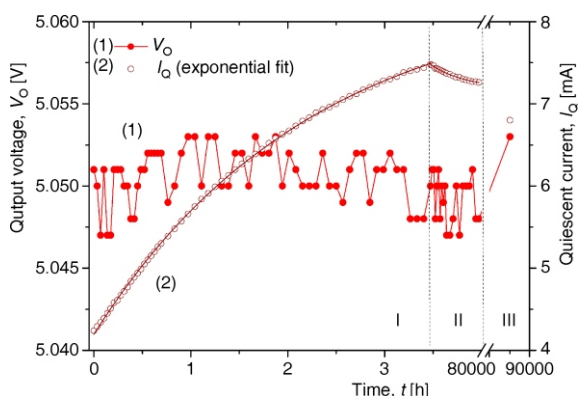
Figure 2. Change in the output voltage and quiescent current in the biased and loaded ($V_{in} = 8$ V, $I_{out} = 100$ mA) voltage regulator L4940V5, under the influence of γ-radiation (area I), followed by the first half an hour after the exposure to γ-radiation (area II), complemented with additional data on 85 000-hour room-temperature annealing without bias (area III); both irradiation and the first ensemble of annealing data for quiescent current were fitted with exponential functions, eqs. (6) and (7)
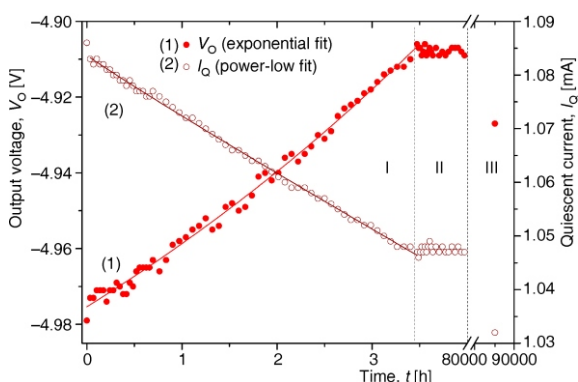

Figure 3. Change in the output voltage and quiescent current in the biased and loaded ($V_{in} = 8$ V, $I_{out} = 100$ mA) voltage regulator LM2990T-5, under the influence of γ-radiation (area I), followed by the first half an hour after the exposure to γ-radiation (area II), complemented with additional data on 85 000-hour room-temperature annealing without bias (area III); irradiation processes were fitted with nearly equal success with both exponential and power-law functions, eqs. (8) and (9)

quasi-low-dropout circuit, LT1086CT5, presented in fig. 4, have a clear declining trend. Both figs. 3 and 4 indicate the operation of moderately loaded voltage regulators LM2990T-5 and LT1086CT5 with a relatively low output voltage, close to the minimum acceptable value of 4.9 V. Whenever it was possible, curves were fitted with linear, exponential or power-law functions.

Data on the output voltage and quiescent current were separated into three parts, in order to unify the data on the irradiation and annealing processes. The first area (I) describes the irradiation period, while the second area (II) in figs. 1-4 is based on data recorded during the initial 30-minute period of the room-tem-
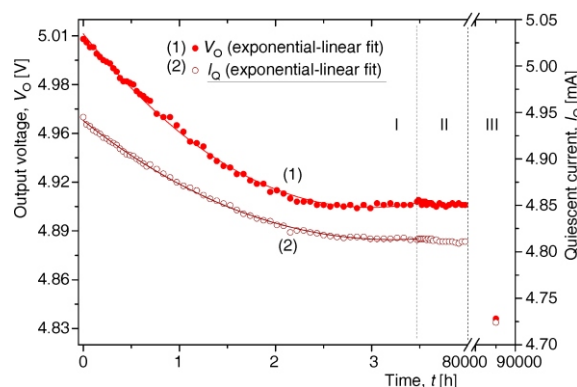

Figure 4. Change in the output voltage and quiescent current in the biased and loaded ($V_{in} = 8$ V, $I_{out} = 100$ mA) voltage regulator LT1086CT5, under the influence of γ-radiation (area I), followed by the first half an hour after the exposure to γ-radiation (area II), complemented with additional data on 85 000-hour room-temperature annealing without bias (area III); irradiation processes were successfully fitted with complex exponential-linear functions, eqs. (10) and (11)

perature annealing, starting immediately after irradiation of the voltage regulators. During the rapid annealing period, variations of the output voltage were negligible and random, without a noticeable trend.

As reported in previously published articles, the LM2940CT5 is a very radiation-sensitive circuit, prone to severe output voltage degradation even after the absorption of relatively low total doses [20, 22, 23]. Yet, this conclusion cannot be drawn from fig. 1, since the increase in output voltage of 0.6%, following the absorption of the total dose of 500 Gy, represents its minor variation. Also, the 10 % decline in the quiescent current for the same dose of 500 Gy is not a sufficient sign of severe degradation. Yet, significant degradation in LM2940CT5 circuits was observed only for much higher output currents, closer to the regulator's nominal current of 1 A [20, 22].

Initial rapid annealing data cannot lead to any clear conclusions on the LM2940CT5 circuit's recovery (fig. 1). Variations in the output voltage of only 2 mV (between 4.986 V and 4.988 V; less than 0.05 % of the nominal output voltage), followed by the variations of quiescent current in the range of just 60 A (between 9.51 mA and 9.57 mA; nearly 0.6 % of the initial quiescent current at the end of irradiation) are really minor, being comparable with the influence of thermal noise on the variations of the measured parameters. Consequently, the data procured during the 30-minute room-temperature annealing of LM2940CT5 circuits is really insufficient to draw any considerable conclusion.

In order to estimate the circuit's characteristics during the irradiation, it was necessary to implement interpolation for the available data set. Variations of the output voltage during irradiation were successfully fitted only with the allometric power-law regression function (being the extension of the classical Freundlich model), presented in the following equation.

160

V. Dj. Vukić.: Rapid and Long-Term Gamma-Radiation Annealing in ...
Nuclear Technology & Radiation Protection: Year 2017, Vol. 32, No. 2, pp. 155-165

$$V_{O_{irr}}^{2940}(t) = 4.95842 - 0.01315\, t^{0.66734} \quad (\overline{R_{pow}^2} = 0.98414) \tag{4}$$

In the LM2940CT5 voltage regulator, quiescent current was successfully fitted with both a linear and a first order exponential function. Nevertheless, the following linear regression function gave slightly better goodness of fit

$$I_{Q_{irr}}^{2940}(t) = 10.515 + 0.288\, t \quad (\overline{R_{lin}^2} = 0.99848) \tag{5}$$

As a primary measure of the goodness of fit in all cases, the adjusted coefficient of determination ($\overline{R^2}$) was used [25]. The adjusted coefficient of determination was presented in parenthesis, behind all the presented regression functions in the paper. In the previous, as well as all the following equations, variations of the measured electrical values were presented as a function of time, expressed in hours. During the irradiation period, time has values between 0 and 3.47222 hours, whilst in the rapid-annealing period, variable t changes between 3.47222 and 3.97222.

In the rapid-annealing period (area II in fig. 1) no noticeable trend (recovery or degrading) could be perceived during the initial 30-minute recovery of biased circuits after irradiation. Finally, after the 85 000-hour room-temperature recovery (area III), while the quiescent current slightly increased, the voltage regulator's output voltage significantly degraded (fig. 1). It is clear that the LM2940CT5 voltage regulator endured high degradation during the 10-year room-temperature annealing, with a nearly critical decline of its output voltage, being only slightly above the minimum acceptable value of 4.9 V.

By contrast with the data for the LM2940CT5 device, from fig. 2 it can be seen that during the irradiation of the L4940V5 voltage regulator, the quiescent current nearly doubled, while the circuit's negative feedback reaction kept an output voltage in close proximity to its initial voltage of 5.05 V. Figure 2 indicates an 80% rise in the quiescent current, with a clearly expressed exponential characteristic, precisely indicating the trend of the quiescent current change. During the irradiation, the output voltage of the L4940V5 voltage regulator was nearly constant, and the same may be said also for the initial 30-minute annealing period (variations of up to 5-6 mV, *i. e.*, only 1 ‰ of the nominal output voltage). Therefore, data on the output voltage are not useful for estimation of the L4940V5 circuit's recovery after the exposure (nevertheless, stable output voltage in all the operating areas is a sign of the voltage regulator's potential high radiation tolerance). On the other hand, a completely different response can be seen in fig. 2, describing the quiescent current change during the initial room-temperature annealing. Both the irradiation data and the first 30 minutes of quiescent current annealing were successfully fitted with exponential functions. The exponential approximations were nearly ideal, since the adjusted coefficients of determination for both rising and declining curves were close to 1. Neither polynomial nor power-law functions could provide such high goodness of fit. Relation (6) presents the first order exponential regression function for the period of irradiation (area I in fig. 2), while eq. (7) describes the annealing period for the L4940V5 voltage regulator (area II)

$$I_{Q_{irr}}^{4940}(t) = 8.379 + 4.185\, e^{\frac{t}{2.245}} \quad (\overline{R_{\exp}^2} = 0.99985) \tag{6}$$

$$I_{Q_{ann}}^{4940}(t) = 7.185 + 4502\, e^{\frac{t}{0.361}} \quad (\overline{R_{\exp}^2} = 0.99613) \tag{7}$$

The implemented approximation of the rapid annealing process (eq. 7) indicates the very fast recovery of the L4940V5 voltage regulator, decreasing the excess quiescent current by nearly 7 % after only 30 minutes of the room-temperature recovery of biased samples. Furthermore, it was expected that the irradiated circuits would be significantly recovered after the elapse of 10 years, regardless of the absence of the input bias voltage. In order to examine said hypothesis, circuits L4940V5 (as well as all the other examined voltage regulators) were tested after 85 000 hours of the room-temperature recovery.

As can be clearly seen from fig. 2, circuit L4940V5 only partially recovered from irradiation, leaving the excess quiescent current of only 17 % less than immediately after irradiation. Nevertheless, the devices were completely functional during both the irradiation and annealing periods.

The data in figs. 3 and 4 indicate similar effects of irradiation and rapid room-temperature annealing on these devices, which are significantly different in terms of construction and circuit topology. Nevertheless, the data describing the influence of long-term annealing on these circuits were completely different, needing further analysis.

Figure 3 presented data on the output voltage and quiescent current in the negative voltage regulator LM2990T-5, with power-law and exponential regression functions for the irradiation process. As in the case of circuit LM2940CT5 and contrary to voltage regulator L4940V5, the rapid-annealing process in the LM2990T-5 circuit could not be fitted with any function, since there was no trend in the primary room-temperature annealing process. On the other hand, data on both the output voltage and quiescent current, procured during the uninterrupted irradiation, were nearly ideally fitted with either linear, exponential or power-law functions. Yet, for the output voltage, exponential model was marginally better than others, while power-law model gave the best goodness of fit for variations of the quiescent current. The first-order

exponential regression functions, describing variations of the output voltage during irradiation of the LM2990T-5 voltage regulator, is presented in eq. (8)

$$V_{O_{irr}}^{2990}(t) \quad 5.093 \quad 0.118e^{\frac{t}{7.538}}$$
$$(R_{exp}^{2} \quad 0.99353)$$
(8)

Allometric power-law function, *i. e.*, extension of the classical Freundlich model ($y = a + bx^c$), being the most successful approximation of the quiescent current variations, is presented in eq. (9)

$$I_{Q_{irr}}^{2990}(t) \quad 10.72794 \quad 1.78744t^{0.48516}$$
$$(R_{pow}^{2} \quad 0.99798)$$
(9)

The long-term annealing process described in fig. 3 indicates a moderate recovery of the output voltage, but further decline of the quiescent current. The negative voltage regulator LM2990T-5 has very low quiescent current (see fig. 3), primarily owing to its serial super-β npn power transistor. Therefore, the significant decline in the quiescent current may indicate the critical decline in the serial transistor's base current, which may further lead to a complete failure of the circuit [21]. Nevertheless, the decline recorded in fig. 3 was not critical for the voltage regulator's proper operation.

The data in fig. 4 were procured during examination of the quasi-low-dropout voltage regulator LT1086CT5 in the γ-radiation field. Unlike all the other tested circuits, these voltage regulators expressed obvious saturation of both the output voltage and quiescent current after absorption of the total dose of 300 Gy (fig. 4). Therefore, none of these values could be successfully fitted using pure exponential functions. Also, neither linear nor power-law regression functions could provide satisfactory goodness of fit. So, variations of both the output voltage and quiescent current in the γ-radiation field were nearly ideally fitted with mixed exponential-linear functions. The complex linear-exponential regression functions, describing variations of the output voltage and quiescent current during irradiation of the LT1086CT5 voltage regulator, are presented in eqs. (10) and (11)

$$V_{O_{irr}}^{1086}(t) \quad 32.193 \quad 0.901t \quad 37.204\, e^{\frac{t}{38.198}}$$
$$(R_{lin\ exp}^{2} \quad 0.99745)$$
(10)

$$I_{Q_{irr}}^{1086}(t) \quad 21.18 \quad 0.754t \quad 26.121e^{\frac{t}{31.27}}$$
$$(R_{lin\ exp}^{2} \quad 0.99873)$$
(11)

In the rapid-annealing area after irradiation, the devices LT1086CT5 were not an exception to most of the other examined low-dropout voltage regulators: there was no expressed recovery of a degradation trend during the first 30 minutes after irradiation.

Yet the data in fig. 4 on the long-term room-temperature annealing clearly demonstrated that the 10-year storage period of the LT1086CT5 circuits was certainly not a recovery, since a sharp degradation of both output voltage and quiescent current was recorded. This was particularly important for the output voltage, since the circuits' output voltage was below the acceptable minimum of 4.9 V even for a moderate load of only 100 mA. Therefore, for a moderate load of some 10 % of the nominal output current, the quasi-low-dropout voltage regulators LT1086CT5 demonstrated the greatest gamma-radiation sensitivity among the four examined types of low-dropout voltage regulators.

In order to evaluate the examined circuits' radiation tolerance, the quiescent current annealing factor was used (eq. 3), being based on the measured values of quiescent current. Therefore, fig. 5 presented data on the quiescent current annealing factor for all four types of examined circuits (LM2940CT5, L4940V5, LM2990T-5 and LT1086CT5). All the data necessary for calculation of the quiescent current annealing factors were presented in figs. 1-4.

Decreasing values of the annealing factor indicate the circuit's recovery, while the increasing value of F_{I_Q} is an indicator of the circuit's further degradation. Thus, fig. 5 is a good illustration of the great differences between the four types of tested voltage regulators. Particularly the long-term annealing process demonstrated completely different responses of low-dropout circuits with serial pnp transistors, on the one hand, and voltage regulators with serial npn transistors, on the other.

Nevertheless, the data in fig. 5 cannot be used for obvious demonstration of the rapid annealing process. So, in fig. 6 the data on the quiescent current were normalised and magnified in order to enable the clear graphical presentation of the first half-hour of the room-temperature annealing process of biased circuits. Figure 6 indicates a decreasing trend of the quiescent current in circuit L4940V5, opposite to the
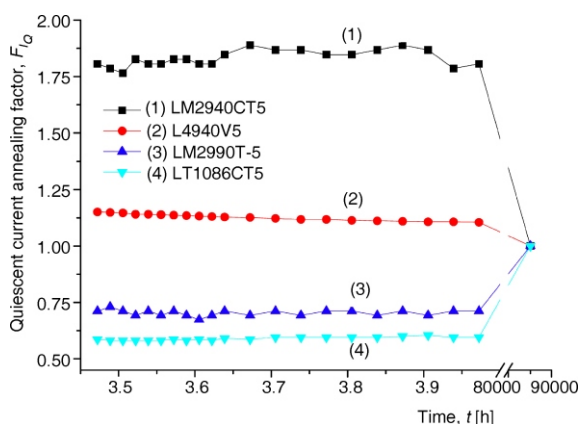

Figure 5. The quiescent current annealing factors in low-dropout voltage regulators during the first 30 minutes after exposure to γ-radiation, as well as following the 10-year room-temperature annealing process

162

V. Dj. Vukić.: Rapid and Long-Term Gamma-Radiation Annealing in ...
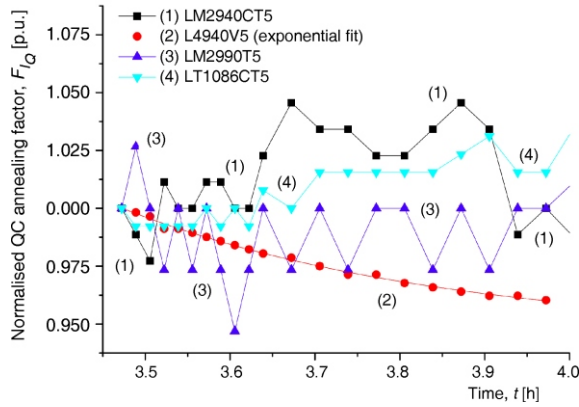Nuclear Technology & Radiation Protection: Year 2017, Vol. 32, No. 2, pp. 155-165

Figure 6. Normalised quiescent current annealing factors in low-dropout voltage regulators, procured during the first 30 minutes after the exposure to γ-radiation

nearly random variations of the other circuits' quiescent current, pointing to the great difference between voltage regulator L4940V5 and all the other examined circuits. The normalised quiescent current annealing factor in the L4940V5 voltage regulator was successfully fitted with the following exponential function

$$F_{I_Q}^{4940}(t) = 0.946 + 534.596 \, e^{-\frac{t}{0.378}}$$

$$(R_{\exp}^2 = 0.99617) \qquad (12)$$

Therefore, figs. 5 and 6, observed together, are a good illustration of both the long-term and rapid annealing processes in all the examined circuits. While in the long-term 10-year period there is a clear difference between devices with pnp and npn serial power transistors, in the short-term half-hour period the circuit L4940V5 distinguishes itself among other devices.

In order to analyse the mentioned differences, now it is necessary to start the additional discussion in order to analyse the perceived radiation and post-irradiation effects.

DISCUSSION

Several different irradiation and annealing periods implemented in the described experiment enabled broad introspection on the radiation and post-irradiation effects in low-dropout voltage regulators. Since the irradiation and annealing were uninterrupted, there were no disruptions in the charge-trapping processes affected by the variations of chip temperature, bias voltage or load current.

Temperature and bias conditions (directly affecting the electric field in the isolation oxide) have a significant influence on the bipolar transistor annealing. The existence of the output voltage at terminals or elevated temperature leads to increase of the carrier mobility, caused by the presence of an electric field or

the thermal excitation. High-quality, thin MOSFET oxides, in general, have the potential for a rapid annealing after irradiation. On the other hand, the thick, field oxides used in bipolar integrated circuits are much more contaminated during the initial processing and therefore tend to trap a much greater quantity of the electric charge. It is generally assumed that field oxides are very radiation-sensitive, while the MOSFET gate oxides are radiation-tolerant. This may not always be true, since recent research indicates that in thick oxides, with low electric fields and at low temperature, the charge yield may be relatively low, since most of the oxide would be a "dead layer" [26], scarcely affected by the radiation-induced charge trapping. Thus, as a consequence, the oxide-trapped charge concentration will be lower than the expected square of oxide thickness [26]. In high-quality MOSFET oxides, with thin gates and, consequently, high electric fields, the concentration of the oxide-trapped charge will be nearly proportional to the square of the oxide thickness ($N_{ot} \sim d_{ox}^2$) [2, 4, 7] or even its third degree ($N_{ot} \sim d_{ox}^3$) [4]. Nevertheless, due to the much lower volume, the total quantity of the oxide-trapped charge in the thin gate oxide will be significantly lower, thus leading to its faster recovery from the influence of ionising radiation. High oxide thickness and impurities contamination clearly point to the potential of a very large quantity of trapped charge in field oxides, especially at higher temperatures and electric fields [26].

The mentioned mechanisms of charge-trapping are fundamental to the observed annealing process, presented in figs. 2 and 6. In the initial phase, annealing of the oxide-trapped charge is dominant in the L4940V5 circuit. The rapid annealing process observed in the L4940V5 voltage regulator is affected by the quality of the implemented field oxide; thus, eq. (7) is the most important regression function obtained in the presented research.

Using the quiescent current as the primary measure of the integrated circuit's radiation tolerance was particularly useful for the rough estimation of the influence of the trapped charge. As stated in the theory section, trapped charge may be divided into interface traps and the oxide-trapped charge. A rise in the concentration of interface traps increases excess base current both in npn and pnp transistors, while in the pnp transistors the interface traps affect the base current rise (and, therefore, the pnp transistor's degradation), whence the oxide-trapped charge (above the base area) suppresses the negative effects of the interface traps [27]. Since the concentration of the oxide-trapped charge increases exponentially with the total dose [28] (contrary to the interface traps concentration, which increases linearly with the absorbed dose [28]), it will cause a sharp exponential rise in the excess base current of the affected npn transistors. Therefore, the quiescent current, as a summary supply

current of all the elementary transistors in the voltage regulator control circuit, will directly replicate the summary effects of the trapped charge in the oxide and at interfaces.

According to the data observed in figs. 1-4 and eq. (7), a procedure for a quick identification of the potential radiation-tolerant voltage regulators may be proposed: after exposure to the total dose of ionising radiation, irradiated circuits have to be left operational, out of the ionising radiation field, at room temperature and with the same bias and load as during the irradiation. The output voltage and quiescent current have to be measured for up to one hour, with time intervals of 60 seconds or less. If the absolute value of the output voltage falls below the threshold of acceptable operation (98 % of the nominal output voltage or a similar value), the voltage regulator is not sufficiently radiation-tolerant. If the output voltage is above the specified threshold and a clear trend of the quiescent current recovery can be observed, a circuit may later prove to be acceptably radiation-tolerant. If no recovery trend can be observed in the quiescent current, or even further degradation is noticed, then the examined voltage regulator is certainly a radiation- sensitive device and cannot be used in radiation environments.

This procedure may also be used in control points, after the absorption of lower doses (*i. e.*, 10-20 % of the predetermined total dose). The proposed up to one-hour time interval is enough for implementation with the existing standards, MIL STD 1019.8 [29] and ESCC 22900 [30], since they schedule up to two-hour intervals between two successive irradiations. The described procedure would be more suitable for a quick identification of the radiation-sensitive components, rather than a sufficient tool for the qualification of potential rad-hard devices. Analogue bipolar integrated circuits, successfully passing the initial rapid-annealing check, should be further analysed according to some of the standards mentioned in this paragraph.

CONCLUSIONS

Low-dropout voltage regulators, integrated circuits with both pnp and npn serial power transistors, were exposed to a total ionising dose of 500 Gy, without cessation of irradiation until the total determined dose was absorbed. Immediately after irradiation, the output voltage and quiescent current of biased and loaded samples were monitored for 30 minutes. In the next step, all the irradiated samples were left in storage for the next 10 years and thereafter tested for the effects of room-temperature annealing.

Circuit LM2940CT5 did not show any rapid-annealing trend, yet demonstrated significant degradation in the output voltage after the 10-year room-temperature annealing. Just as in the case of circuit LM2940CT5, the negative voltage regulator LM2990T-5 expressed a significant decline in the quiescent current, but the opposite trend of the (absolute value of) output voltage. The quasi-low-dropout voltage regulator LT1086CT5 expressed a clear decline in both the output voltage and quiescent current. Both circuits with serial npn transistors, LM2990T-5 and LT1086CT5, demonstrated a significant decline in the output voltage, approaching the minimum acceptable (absolute) value of output voltage, being 4.9 V. The positive voltage regulators L4940V5 did not express significant variations in the output voltage either during exposure to ionising radiation or during any phase of the annealing process. Nevertheless, the increase in the quiescent supply current was sharp, although it did not affect the circuit's proper operation.

Whenever existed significant change in voltage regulators' output voltage and quiescent current, these variations were successfully fitted with exponential, power-law and linear regression functions. During the rapid-annealing period of biased circuits, only devices L4940V5 demonstrated any trend that could be fitted with a regression function, and were, nearly ideally, fitted with the first-order decreasing exponential function. Immediately after exposure to ionising radiation, all the other voltage regulators expressed indeterminate variations in the quiescent supply current. In all cases, the implemented regression functions were nearly ideal, since the adjusted coefficient of determination (R^2) always had values exceeding 0.984.

Ten-year room-temperature annealing showed up the circuit degradation of the moderately loaded devices LM2940CT5 and LT1086CT5, which was not clearly noticeable immediately after absorption of the total dose of 500 Gy. Long-term annealing also indicated the LM2990T-5 circuit's marginal radiation tolerance and, finally, the high radiation-hardness of the L4940V5 voltage regulator for total ionising doses up to 500 Gy.

The quiescent current annealing factor (F_{I_Q}) was introduced as an alternative measure of the voltage regulator's recovery from the influence of γ-radiation. For all four types of voltage regulators, values of the quiescent current annealing factor were presented, for both the rapid and long-term annealing periods.

Wide variations of the quiescent current in the L4940V5 voltage regulator led to identification of a new procedure for estimation of the radiation-hardness of the examined integrated voltage regulators, planned for operation in the radiation environment. In short, after exposure to the total dose of ionising radiation, the irradiated circuits have to be left operational, out of the ionising radiation field, with the same temperature, bias and load as during the irradiation. If a clear trend of the quiescent current's recovery can be observed, a circuit may later prove to be acceptably radiation-tolerant. If no recovery trend can be observed within the first hour after irradiation, or even further degradation is noticed, then the examined voltage reg-

164

V. Dj. Vukić.: Rapid and Long-Term Gamma-Radiation Annealing in ...
Nuclear Technology & Radiation Protection: Year 2017, Vol. 32, No. 2, pp. 155-165

ulator is a radiation-sensitive device and cannot be used in radiation environments.

The proposed procedure may also be used for other kinds of linear bipolar integrated circuits, such as operational amplifiers, comparators and voltage references. The essential idea is to use the circuit's quiescent supply current as the primary measure of the circuit's degradation or recovery in the radiation environment.

ACKNOWLEDGEMENT

REFERENCES

[1] Messenger, G. C., Ash, M. S., The Effects of Radiation on Electronic Systems, Van Nostrand Reinhold, 1992

[2] Holmes-Siedle, A., Adams, L., Handbook of Radiation Effects, Oxford University Press, New York, USA, 2004

[3] Pease, R. L., Total Ionizing Dose Effects in Bipolar Devices and Circuits, *IEEE Trans. Nucl. Sci., 50* (2003), 3, pp. 539-551

[4] Hughes, H. L., Benedetto, J. M., Radiation Effects and Hardening of MOS Technology: Devices and Circuits, *IEEE Trans. Nucl. Sci., 50* (2003), 3, pp. 500-521

[5] Jakšić, A. B., *et al*., Isothermal and Isochronal Annealing Experiments on Irradiated Commercial Power VDMOSFET, *IEEE Trans. Nucl. Sci., 47* (2000), 3, pp. 659-666

[6] Ristić, G. S., *et al*., The Isochronal Annealing of Irradiated *n*-Channel Power VDMOSFET, *Nucl. Instr. Meth. Phys. Res. B, 366* (2016), Jan., pp. 171-178

[7] Oldham, T. R., McLean, F. B., Total Ionizing Dose Effects in MOS Oxides and Devices, *IEEE Trans. Nucl. Sci., 50* (2003), 3, pp. 483-499

[8] Chen, X. J., *et al*., Post-Irradiation Annealing Mechanisms of Defects Generated in Hydrogenated Bipolar Oxides, *IEEE Trans. Nucl. Sci., 55* (2008), 6, pp. 3032-3038

[9] Barnes, R. L., *et al*., Post Irradiation Effects (PIE) in Integrated Circuits, *IEEE Trans. Nucl. Sci., 39* (1992), 3, pp. 328-341

[10] Bielejec, E., *et al*., Metrics for Comparison Between Displacement Damage Due to Ion Beam and Neutron Irradiation in Silicon BJT, *IEEE Trans. Nucl. Sci., 54* (2007), 6, pp. 2282-2287

[11] Dhombres, S., *et al*., Study of a Thermal Annealing Approach for Very High Total Dose Environments, *IEEE Trans. Nucl. Sci., 61* (2014), 6, pp. 2923-2929

[12] Djorić-Veljković, S. M., *et al*., Annealing of Radiation-Induced Defects in Burn-In Stressed Power VDMOSFET, *Nucl Technol Radiat., 26* (2011), 1, pp. 18-24

[13] Pejović, M. M., Processes in Radiation Sensitive MOSFET During Irradiation and Post Irradiation Annealing Responsible for Threshold Voltage Shift, *Rad. Phys. Chem., 130* (2017), Jan., pp. 221-228

[14] Blamires, N. G., *et al*., pMOS Dosimeters: Long-Term Annealing and Neutron Response, *IEEE Trans. Nucl. Sci., 33* (1986), 6, pp. 1310-1315

[15] Pejović, M. M., *et al*., Successive Gamma-Ray Irradiation and Corresponding Post-Irradiation Annealing of pMOS Dosimeters, *Nucl Technol Radiat., 27* (2012), 4, pp. 341-345

[16] Oldham, T. R., *et al*., Post-Irradiation Effects in Field-Oxide Structures, *IEEE Trans. Nucl. Sci., 34* (1987), 6, pp. 1184-1189

[17] Fleetwood, D. M., Total Ionizing Dose Effects in MOS and Low-Dose-Rate-Sensitive Linear Bipolar Devices, *IEEE Trans. Nucl. Sci., 60* (2013), 3, pp. 1706-1730

[18] Gregory, B. L., Sander, H. H., Injection Dependence of Transient Annealing in Neutron-Irradiation Silicon Devices, *IEEE Trans. Nucl. Sci., 14* (1967), 6, pp. 116-126

[19] Vukić, V. Dj., Osmokrović, P. V., Impact of the Excess Base Current and the Emitter Injection Efficiency on Radiation Tolerance of a Vertical pnp Power Transistor in a Voltage Regulator, *Informacije MIDEM, 43* (2013), 1, pp. 27-40

[20] Vukić, V., Osmokrović, P., Impact of Forward Emitter Current Gain and Geometry of pnp Power Transistors on Radiation Tolerance of Voltage Regulators, *Nucl Technol Radiat., 25* (2010), 3, pp. 179-185

[21] Vukić, V. Dj., Osmokrović, P.V., Failure of the Negative Voltage Regulator in Medium-Photon-Energy X Radiation Fields, *Microelectron. Reliab., 54* (2014), 1, pp. 79-89

[22] Vukić, V., Osmokrović, P., Power Lateral pnp Transistor Operating with High Current Density in Irradiated Voltage Regulator, *Nucl Technol Radiat., 28* (2013), 2, pp. 146-157

[23] Vukić, V., Osmokrović, P., On-Line Monitoring of Base Current and Forward Emitter Current Gain of Voltage Regulator's Serial pnp Transistor in Radiation Environment, *Nucl Technol Radiat., 27* (2012), 2, pp. 152-164

[24] Vukić, V., Influence of Exploitation Conditions on Characteristics of Voltage Regulators, M. Sc. thesis, University of Belgrade (in Serbian), 2005

[25] Theil, H., Economic Forecasts and Policy, North-Holland, Amsterdam, The Netherland, 1961

[26] Johnston, A. H., *et al*., Field Dependence of Charge Yield in Silicon Dioxide, *IEEE Trans. Nucl. Sci., 61* (2014), 6, pp. 2818-2825

[27] Schmidt, D. M., *et al*., Modelling Ionizing Radiation Induced Gain Degradation of the Lateral PNP Bipolar Junction Transistor, *IEEE Trans. Nucl. Sci., 43* (1996), 6, pp. 3032-3039

[28] Pershenkov, V. S., *et al*., The Effect of Emitter Junction Bias on the low-Dose-Rate Radiation Response of Bipolar Devices, *IEEE Trans. Nucl. Sci., 44* (1997), 6, pp. 1840-1848

[29] ***, MIL-STD 883H, Method 1019.8: Ionizing Radiation (Total Dose) Test Procedure, United States Department of Defense; Feb. 26, 2010

[30] ***, ESA European Space Components Coordination. Total Dose Steady-State Irradiation Test Method, ESCC Basic Specification No. 22900, Issue 4, Oct. 2010

Владимир Ђ. ВУКИЋ

БРЗ И ДУГОТРАЈАН ОПОРАВАК ОД УТИЦАЈА ГАМА-ЗРАЧЕЊА СТАБИЛИЗАТОРА СА НИСКИМ ПАДОМ НАПОНА

Узорци две врсте стабилизатора са ниским падом напона, са редним пнп и нпн транзисторима, испитани су у условима изотермног опоравка од утицаја гама-зрачења на собној температури. Након беспрекидног апсорбовања укупне дозе јонизујућег зрачења од 500 Gy, поларизовани и оптерећени стабилизатори напона су испитани приликом опоравка на собној температури током првих тридесет минута након престанка излагања зрачењу. Поред непрекидног надзора излазног напона и струје према маси непосредно након излагања зрачењу, спроведена су и мерења након десетогодишњег спонтаног опоравка узорака на собној температури. Резултати добијени приликом озрачивања и брзог опоравка стабилизатора напона апроксимирани су линеарним, експоненцијалним и степеним регресионим функцијама. Предложена је једноставна процедура, заснована на фактору опоравка струје према маси, намењена за брзу естимацију радијационе отпорности стабилизатора напона током пострадијационог изотермног опоравка. Да би могла да буде процењена радијациона отпорност интегрисаног кола, одмах након озрачивања испитивани узорци треба да остану у истим радним условима као и приликом излагања зрачењу. Ако се уочава јасан тренд опоравка струје према маси, коло може да буде подвргнуто додатним испитивањима да би се утврдило да ли је довољна радијациона отпорност. Ако не може да се уочи никакав тренд опоравка кола током првог часа након озрачивања, или ако се уочи његова додатна деградација, онда је испитивани стабилизатор напона радијационо осетљива компонента и не може да се користи у радијационом окружењу. Описана процедура се заснива на макроскопским радијационим ефектима, захвата наелектрисања у изолационим оксидима и граничним површинама интегрисаних кола.

Кључне речи: стабилизатор напона, гама зрачење, струја према маси, фактор опоравка, изотермни опоравак, пострадијациони ефекат, регресиона анализа